



Communication

Dynamic and reversible electrowetting with low voltage on the dimethicone infused carbon nanotube array in air



Miao Wang^{a,1}, Lei Zhou^{a,1}, Yaqi Hou^{b,1}, Wen He^b, Wei Liu^a, Feng Wu^a, Xu Hou^{a,b,*}

^a Research Institute for Biomimetics and Soft Matter, Fujian Provincial Key Laboratory for Soft Functional Materials Research, Jiujiang Research Institute, College of Physical Science and Technology, Xiamen University, Xiamen 361005, China

^b State Key Laboratory of Physical Chemistry of Solid Surfaces, Collaborative Innovation Center of Chemistry for Energy Materials, College of Chemistry and Chemical Engineering, Xiamen University, Xiamen 361005, China

ARTICLE INFO

Article history:

Received 8 April 2020

Received in revised form 28 April 2020

Accepted 30 April 2020

Available online 8 May 2020

Keywords:

Carbon nanotube array

Electrowetting

Reversible

Dynamic

Low voltage

ABSTRACT

Unremitting efforts have been intensively making for pursuing the goal of the reversible transition of electrowetting owing to its vital importance to many practical applications, but which remains a major challenge for carbon nanotubes due to the irreversible electrochemical damage. Herein, we proposed a subtly method to prevent the CNT array from electrochemical damage by using liquid medium instead of air medium to form a liquid/liquid/solid triphase system. The dimethicone dynamically refills in CNT arrays after removing of voltage that makes the surface back to hydrophobic, which is an elegant way to not only decrease energy dissipation in electrowetting process but also obtain extra energy in reversible dewetting process. Repeated cycles of *in situ* experiments showed that more than four reversible electrowetting cycles could be achieved in air. It worth mention that the *in situ* reversible electrowetting voltage of the dimethicone infused CNT array has been lowered to 2V from 7V which is the electrowetting voltage for the pure CNT array. The surface of the dimethicone infused CNT array can maintain hydrophobicity with a contact angle of 145.6° after four cycles, compared with 148.1° of the initial state. Moreover, a novel perspective of theoretical simulations through the binding energy has been provided which proved that the charged CNTs preferred binding with water molecules thereby replacing the dimethicone molecules adsorbed on the CNTs, whereas reconnected with dimethicone after removing the charges. Our study provides distinct insight into dynamic reversible electrowetting on the nanostructured surface in air and supplies a way for precise control of wettability in surface chemistry, smart phase-change heat transfer enhancement, liquid lenses, microfluidics, and other chemical engineering applications.

© 2020 Chinese Chemical Society and Institute of Materia Medica, Chinese Academy of Medical Sciences.

Published by Elsevier B.V. All rights reserved.

Dynamic control of surface wettability showed great significance to many chemical and engineering fields [1], such as surface chemistry [2], enhanced phase-change heat transfer [3–8], liquid lenses [9–12], etc. Electrowetting triggered by the stimuli electric is an effective approach to temporarily change the surface wettability through the spread of a potential-induced droplet. Carbon nanotube (CNT) array has the advanced features of typical nanostructured surface and excellent hydrophobicity properties, and which can wet the droplet on their surface through the

application of voltage and achieve rapid electrowetting switch [1,13–16]. However, achieving reversible electrowetting on the surface of CNT arrays in the air remains a big challenge due to the electrochemical damage [17,18]. There are currently three possible reasons for the mechanism of the change in interface energy between multi-walled carbon nanotubes and liquids after an electric field is applied. The first reason is that the energy barrier entering the carbon nanotubes improves the stability of the hydrogen bonds among the water molecules in the carbon nanotubes, which is beneficial to increasing the water flux of the carbon nanotubes, thereby increasing the wettability [19–21]. The second reason is that after applying a certain amount of electric field, oxygen or oxygen-containing molecules are combined with carbon nanotubes and form carbon oxide tubes. The oxygen atoms either enter crystal hole defects on the surface of the carbon tube or are adsorbed into Stone-Wales defects [22]. Both of these causes can lead to an increase in the surface binding forces of

* Corresponding author at: Research Institute for Biomimetics and Soft Matter, Fujian Provincial Key Laboratory for Soft Functional Materials Research, Jiujiang Research Institute, College of Physical Science and Technology, Xiamen University, Xiamen 361005, China.

E-mail address: houx@xmu.edu.cn (X. Hou).

¹ These authors contributed equally to this work.

water molecules with carbon nanotubes, making hydrophobic surface of the carbon nanotube array hydrophilic. The third one is that an external electric field can bring some oxygen-containing functional groups, such as $-\text{OH}$ or $-\text{COOH}$, to be grafted on carbon nanotubes. These functional groups can change the surface properties of the carbon nanotubes showing an increasing wettability of water molecules [19,23].

In fact, there are two strategies to realize the reversibility of electrowetting, one is decreasing energy dissipation during the wetting process, and the other is providing additional energy during dewetting process. The method of introducing energy includes high temperature [24], ultrasound [25], electrolysis [26] and oscillation [27]. The method of reducing energy dissipation includes creating an oil environment [28] or electrowetting on oil-infused electrode [29]. For carbon nanotube arrays, the structural breakage caused by electrowetting require introducing extra energy in the dewetting process, such as high-temperature annealing in vacuum [23,30–32] or combination of UV [32–34] and ozone [23,35]. Using liquid medium is a recent method to obtain extra energy for reversible electrowetting, but it was achieved in the oil phase while not in the air [36,37].

Here, we show a dynamic strategy of infusing an appropriate amount of dimethicone in pristine CNT array. The infused dimethicone can prevent the CNT array from electrochemical damage and dynamically refill in CNT arrays after removing of voltage, which makes the surface recover to hydrophobic. The oil layer on the surface of the dimethicone infused carbon nanotube array reduces dissipation in the wetting process, while the three-phase system of liquid/liquid/solid built on the surface of the rough nanostructure provides additional energy in the dewetting process. By regulating the amount of dimethicone and the magnitude of the voltage, we have achieved that more than four reversible electrowetting cycles can be performed *in situ*. The theoretical simulations further revealed that the charged CNTs preferred to binding with water molecules thereby replacing the dimethicone molecules adsorbed on the CNTs.

A schematic of the electrowetting experiment is shown in Fig. 1a, where the dimethicone is seen infusing and wrapping in the CNT array. The effects of critical parameters like the infiltration amount and size of the droplet have been optimized after systematically studies to reduce the difference between the energy at the liquid-dimethicone and CNT-liquid interface. Accordingly, Fig. 1b shows the profile of the dimethicone infused CNT array which was taken by the shape measurement laser microscope because it contains a liquid phase. It can be seen that the dimethicone did fill the gaps of the CNT array uniformly and wrapped the carbon nanotubes. From the side altitude morphology on the right, the CNT array is well oriented, and the dimethicone

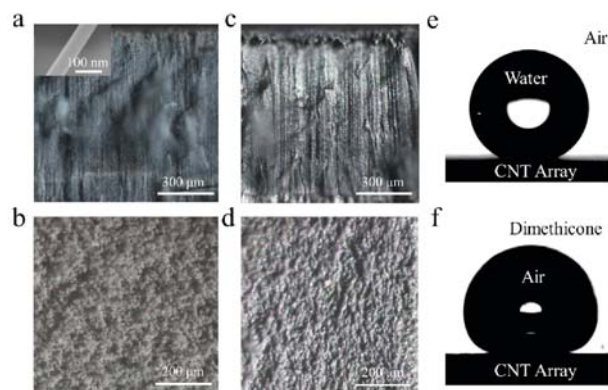


Fig. 2. Fluorescence micrographs and contact angle images. The cross-section (a) (inset: magnified TEM image shows the diameter of a CNT) and top surface (b) micrographs of CNT array. The cross-section (c) and top surface (d) micrograph of dimethicone infused CNT array. (e) The contact angle of deionized water on CNT array in air. (f) The contact angle of the air bubble on the CNT array in dimethicone.

coating is very smooth, without overflowing or damaging the shape of the carbon nanotubes.

Figs. 2a and b are fluorescence micrographs of the side and surface morphologies of the CNT array. Correspondingly, the morphologies after infiltration with dimethicone are shown in Figs. 2c and d. It can be seen that after infusing appropriate amount of dimethicone in CNT array, the dimethicone does not sink down to the bottom of the CNT array, but fills the gaps of the CNT array and covers the CNTs, resulting in a reduction of the surface roughness. Reflective dimethicone can be seen on the surface and side of the CNT array, which is evenly soaked. For the subsequent electrowetting experiments, we tested the contact angles of deionized water and dimethicone on the surface of the CNT array. The average contact angle of the deionized water droplets on the surface of the CNT array was 153° (Fig. 2e), which exhibits superhydrophobic properties in air. Since the CNT array is lipophilic to dimethicone, we used the bubble method by inverting the CNT array in the dimethicone and punching an air bubble on the surface of the CNT array to test the average contact angle. The average contact angle of the air bubble on the CNT array in dimethicone was 43.6° (Fig. 2f). The results showed that the CNT array is lipophilic to dimethicone while hydrophobic to water in the air.

In order to demonstrate the electrowetting process on the pristine CNT array, we conducted in-depth experimental research

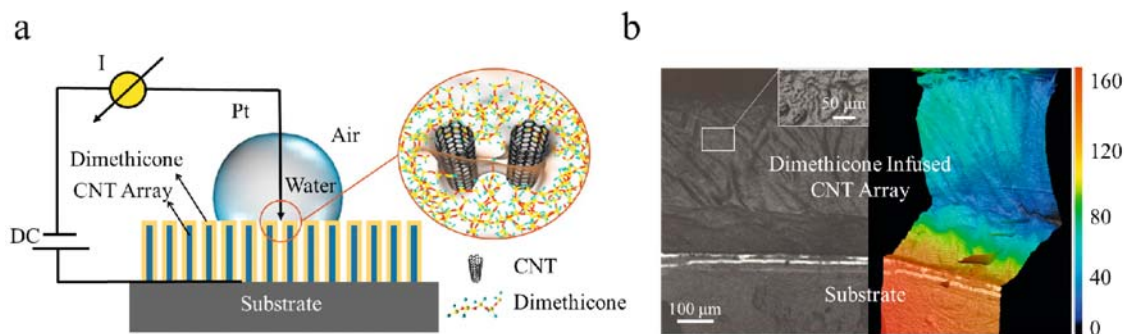


Fig. 1. The electrowetting of droplet on the surface of dimethicone infused CNT array. (a) The schematic of electrowetting on the dimethicone infused CNT array in air. The platinum wire was inserted in the droplet to serve as the cathode. The silicon substrate was acted as the anode. (b) Cross-section morphology image of the dimethicone infused CNT array taken by shape measurement laser microscopy system. The unit of the colorbar is $1 \mu\text{m}$.

on electrowetting at parameters of different array thicknesses and voltages (Figs. S1–S3 in Supporting information). It worth noted that the electrowetting voltage of pristine CNT array was 7 V. From the results, we have divided the electrowetting process of the water droplet on the pristine CNT array into three dynamic steps. In the first step, the contact angle of the droplet was reduced to a saturation value at a relatively rapid speed, and the contact area with the surface was slightly enlarged. In the second step, the contact angle was saturated and decreased slowly. In the third step, the contact area between the droplet and the surface began to expand, and then the droplet sank significantly. The sinking caused the contact angle to shrink rapidly until the droplet disappeared. The time required for the liquid droplet to sink completely decreases with the increase of the applied DC voltage, and the saturated contact angle in the electrowetting process decreases with the increase of the applied DC voltage as well. At the same voltage, the thicker array had a larger saturated contact angle than that of the thinner array, but it took a shorter time for the thicker array to complete the electrowetting process.

Then, the reversible electrowetting experiment of the water droplets on dimethicone infused CNT array was done using the same optimized parameters above. The electrowetting switch process and mechanism are shown in Fig. 3a. At zero voltage, the lower surface tension of the non-polar dimethicone made it coat on CNTs resulting in no wetted by the deionized water droplet. According to the zero-charge potential, the solid-liquid interface has the maximum energy without the accumulated charge. When a sufficient voltage of 2 V is applied between the bottom of the CNT array and the platinum electrode inserted in the water droplet, an electric double layer is formed at the solid/liquid interface and accumulates charge. Therefore, the solid-liquid interface tension will be reduced because of the accumulation of charge. When the surface tension between water and the CNTs is inferior to that between dimethicone and CNTs, the dimethicone is pushed away from the gap between the CNTs. The water partially took place the dimethicone and contacted directly with the surface of the CNTs and electrowetting occurred. At the same time, there was still some dimethicone remained in the gap of the array due to capillary forces, which makes the dynamic recovery possible. After the

voltage was removed, the charge density at the solid-liquid interface went back to zero, and the surface tension between water and CNTs became larger than that between dimethicone and CNTs again. Therefore, the surface of CNTs was recoated by dimethicone and the dimethicone infused CNT array restored to be hydrophobicity. This low voltage electrowetting is attributed to the contact interface transformation from liquid-solid interface to the liquid-liquid interface [37]. For liquid-solid interface, the pinning force is strong; however, the liquid-liquid interface effectively eliminates pinning points, which provides a pathway for free displacement of the droplet with low contact line pinning, leading to superior reversibility with lower driving voltage [38–40]. In order to better observe the entire dynamic process of electrowetting more clearly, we dyed the water red to distinguish it from dimethicone, and recorded a high-definition video of the whole process, of which representative photos are taken and shown below the mechanism in Fig. 3a. It can be seen that when the voltage was applied, the water drained the dimethicone gradually and finally wetted the CNT array. After the voltage was removed, the dimethicone recovered infiltration and the surface become hydrophobic again.

Moreover, the dimethicone infiltration masses in different volumes of CNT array is shown in Fig. 3b. The infiltration mass increased linearly with the volume of the CNT array. Fig. 3c shows the contact angles in four cycles of electrowetting reversible test. Before electrowetting, the contact angle of the droplets on the surface of the dimethicone infused CNT array is about 148.1° . After repetitive and *in-situ* electrowetting for four cycles, the contact angles were 147.9° , 146.8° , 145.1° , 145.6° respectively. Also, multiple tests at three positions on the CNT array were performed, and the trends were the same (Figs. S4–S6 in Supporting information). The results show that the surface of the CNT array after infusing dimethicone achieves reversible conversion between hydrophilic and hydrophobic. Importantly, after more than four times repetition, the surface hydrophobic properties did not decline. The second cycle was performed directly without recovery time.

To further investigate the variation of interactions between CNT surfaces and different liquids (water and dimethicone) before and after the CNT accumulates charges due to the applied voltage, we built the models of the composites of CNTs with water and

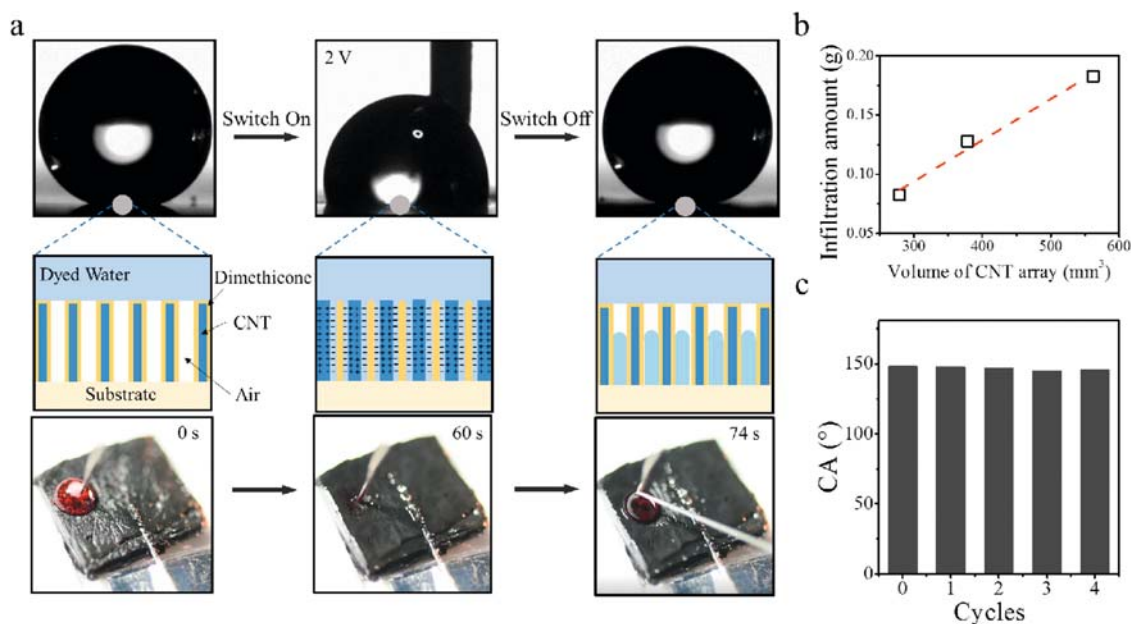


Fig. 3. The reversible electrowetting mechanism and properties. (a) Optical photos of contact angle and relevant schematic mechanism of electrowetting on the surface of CNT array infused with dimethicone. The corresponding images from video of electrowetting process were shown below the mechanism schematic. The applied voltage was 2 V. (b) Dependence of the mass of dimethicone infiltration on the volume of CNT array. (c) *In situ* contact angle with four cycles of reversible electrowetting.

dimethicone, then we compared the binding energies of CNT surface with different liquids and described how the binding energies change after the voltage was applied. All the simulations were performed using LAMMPS molecular dynamics simulator [41]. In the experiments, water molecules and dimethicone molecules moved into the gaps among CNTs and interacted with the surfaces of CNTs. To simulate this process, we built simulation models as shown in Figs. 4a and b. Two CNTs are fixed in the centre of the modelling systems and be frozen during the entire simulations (Table S1 in Supporting information). Around two CNTs, it is full of liquid molecules: water molecules and dimethicone molecules.

In experiments, CNT array acted as the positive electrode. Correspondingly, in the simulations, we assigned different amounts of positive charge ($q = +0|e|$, $+5|e|$, $+10|e|$) on CNT to reveal the different voltages which are applied in experiments. The binding energies between different liquids molecules (water and dimethicone) can be calculated according to Eq. 1.

$$E_{\text{absorption}} = \Delta E = E_{\text{liquid/CNT}} - (E_{\text{liquid}} + E_{\text{CNT}}) \quad (1)$$

In dynamic simulations, two CNTs were fixed, therefore the total energy of CNT is constant. The binding energies due to the adsorption of liquid molecules to the surface of CNTs are reflected in the difference between the equilibrium energy of the composite system and the equilibrium energy of the pure liquids. Based on this, we simulated the NVT dynamic equilibrium process of the pure water, the pure dimethicone and the composite systems with different charged CNTs. The parameters of the systems are listed in Table S1, and the force field parameters adopted are displayed in Tables S2 and S3 (Supporting information) [42–44]. More details of the simulation settings are described in Supporting information.

The energy variations over simulation time are shown in Fig. 4a and b. As can be seen, during the equilibrium processes of the two systems, the energy decreases rapidly and gradually approach an equilibrium value which fluctuates up and down. This equilibrium value is the energy of the current system. Comparing the two graphs, when CNTs are added, the energy of the dimethicone system increases while the energy of the water system decreases. This shows that water molecules are more easily adsorbed to the surface of the CNTs than that of dimethicone.

To better compare the energy changes in the two systems of water and dimethicone, we calculated the energy change (ΔE) of the composite system after adding the CNTs, that is, the strength of the binding energy, as shown in Fig. 4c. It shows that the binding energy of the dimethicone system is a positive value of 647.304 kcal/mol; the binding energy of the water system is a negative value of -118.172 kcal/mol. At the same time, with the increase in the number of positive charges on the surface of the CNTs, the binding energies of the dimethicone systems are almost unchanged, while the binding energies of the water molecule systems are further reduced. When the surface charge of the CNTs reaches 10e, the binding energy of water molecules to the CNTs can reach up to -471.420 kcal/mol, which is 3.99 times the binding energy of uncharged CNTs (-118.172 kcal/mol). When CNTs adsorb water molecules, the energy change of entire system is a negative value, which means the energy of the entire system goes down when water molecules adsorb onto the CNTs; On the contrary, when dimethicone molecules are adsorbed, the total energy of the entire system tends to go up, the energy change is a positive value. As we know, equilibrium system tends to the most stable structure with the lowest energy. Therefore, the CNT surface is more likely to adsorb water molecules instead of dimethicone molecules. Also, the simulation data shows that when the CNTs were charged due to the applied voltage, the binding energies with water molecules are greatly increased, which further promotes the CNTs to preferentially bind with water molecules, thereby replacing the dimethicone molecules adsorbed on the CNTs and showing wettability of water molecules.

In summary, a dynamic strategy has been developed by infusing an appropriate amount of dimethicone in pristine CNT array, which could prevent the CNT array from electrochemical damage meanwhile lower the energy input. We achieved more than four reversible *in situ* electro-wetting cycles at three positions in the air with the applying voltage of 2 V, and the surface of dimethicone infused CNT array can maintain hydrophobic with a contact angle of 145.6°. A perspective of the theoretical simulation about surface binding energy for electro-wetting was proposed which validates the experimental results well. This work may pave the way for adroit control of dynamic surface wettability changes in relevant smart chemical engineering fields.

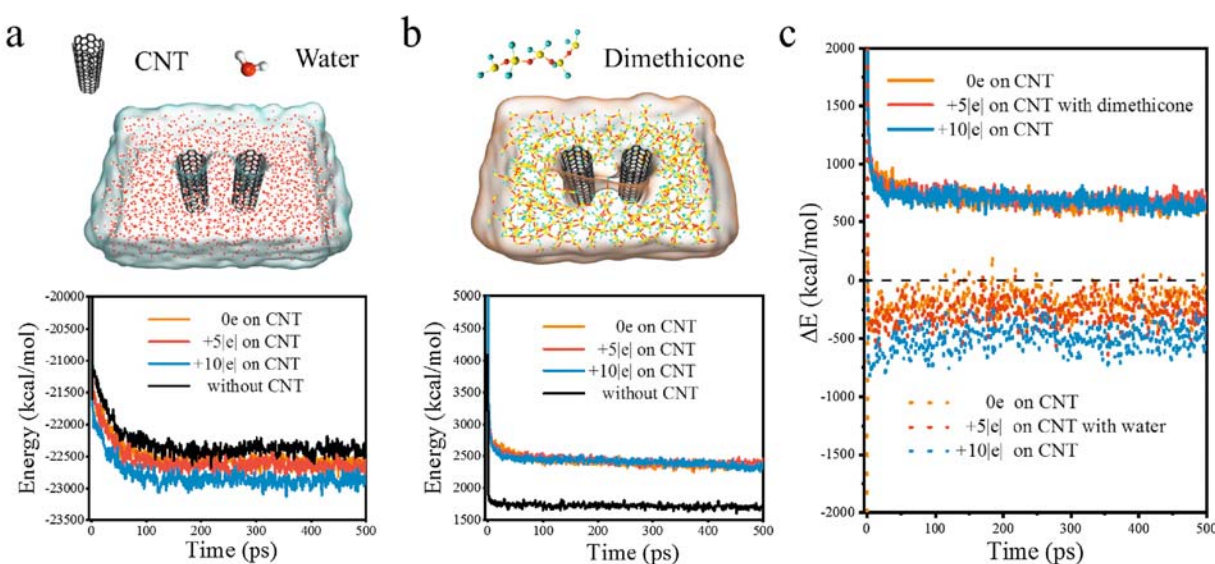


Fig. 4. The schematic of two modelling systems and the corresponding energy variations during the dynamic simulations. (a) CNT array surrounding with water molecules. (b) CNT array surrounding with dimethicone molecules. (c) Comparison of binding energies in charged (uncharged) CNTs/water systems and charged (uncharged) CNTs/dimethicone systems.

Declaration of competing interest

The authors declare that they have no known competing financial interests or personal relationships that could have appeared to influence the work reported in this paper.

Acknowledgments

This work was supported by the National Natural Science Foundation of China (Nos. 51706191, 21673197, 21621091, 21975209), the National Key R&D Program of China (No. 2018YFA0209500), the Fundamental Research Funds for the Central Universities (No. 20720190037) and the Natural Science Foundation of Fujian Province of China (No. 2018J06003).

Appendix A. Supplementary data

Supplementary material related to this article can be found, in the online version, at doi:<https://doi.org/10.1016/j.ccl.2020.04.059>.

References

- [1] M. Liu, L. Jiang, *Adv. Funct. Mater.* 20 (2010) 3753–3764.
- [2] U.N. Tohgha, E.L. Alvino, C.C. Jarnagin, S.T. Iacono, N.P. Godman, *ACS Appl. Mater. Interfaces* 11 (2019) 28487–28498.
- [3] P. Tao, W. Shang, C. Song, et al., *Adv Mater.* 27 (2015) 428–463.
- [4] D.J. Preston, D.L. Mafra, N. Miljkovic, J. Kong, E.N. Wang, *Nano Lett.* 15 (2015) 2902–2909.
- [5] B. Mondal, M. Mac Giolla Eain, Q. Xu, et al., *ACS Appl. Mater. Interfaces* 7 (2015) 23575–23588.
- [6] H. Seo, H.D. Yun, S.Y. Kwon, I.C. Bang, *Nano Lett.* 16 (2016) 932–938.
- [7] C. Yang, C. Chang, C. Song, et al., *Appl. Therm. Eng.* 95 (2016) 445–453.
- [8] G. Zhang, Y.T. Xu, Z. Duan, et al., *Appl. Surf. Sci.* 454 (2018) 262–269.
- [9] J.Q. Wang, H.Y. Wang, X.Y. Li, Y.L. Zi, *Nano Energy* 66 (2019) 104140.
- [10] L.Y. Li, R.Y. Yuan, J.H. Wang, L. Li, Q.H. Wang, *Sci. Rep.* 9 (2019) 13062–13068.
- [11] J. Lee, Y. Park, S.K. Chung, *Sens. Actuators A -Phys.* 287 (2019) 177–184.
- [12] S.L. Li, Z.Q. Nie, Y.T. Tian, C. Liu, *Micromachines* 10 (2019) 515–523.
- [13] W. Cui, H. Ma, B. Tian, Y. Ji, F. Su, *J. Mater. Sci.* 51 (2016) 4031–4036.
- [14] Z. Wang, Y. Ou, T.M. Lu, N. Koratkar, *J. Phys. Chem. B* 111 (2007) 4296–4299.
- [15] D.L. Tian, L.L. He, L. Jiang, *Electric-responsive superwetting surface*, in: A. Hozumi, L. Jiang, H. Lee, M. Shimomura (Eds.), *Stimuli-Responsive Dewetting/Wetting Smart Surfaces and Interfaces*, Springer, Berlin, 2018, pp. 107–132.
- [16] B.A. Kakade, *Nanoscale* 5 (2013) 7011–7016.
- [17] M.E. Kavousanakis, N.T. Chamakos, K. Ellinas, et al., *Langmuir* 34 (2018) 4173–4179.
- [18] J. Heikenfeld, M. Dhindsa, J. Adhes. *Sci. Technol.* 22 (2008) 319–334.
- [19] S. Zhou, J. Sheng, Z. Yang, X. Zhang, *J. Mater. Chem. A* 6 (2018) 8763–8771.
- [20] J. Sheng, Q. Zhu, X. Zeng, Z. Yang, X. Zhang, *ACS Appl. Mater. Interfaces* 9 (2017) 11009–11015.
- [21] J.Y. Li, X.J. Gong, H.J. Lu, et al., *Proc. Natl. Acad. Sci.* 104 (2007) 3687–3692.
- [22] Z.K. Wang, L.J. Ci, L. Chen, et al., *Nano Lett.* 7 (2007) 697–702.
- [23] A.I. Aria, M. Gharib, *J. Vis. Exp.* 74 (2013) e50378–e50386.
- [24] T.N. Krupenkin, J.A. Taylor, E.N. Wang, et al., *Langmuir* 23 (2007) 9128–9133.
- [25] J.B. Boreyko, C.H. Chen, *Phys. Rev. Lett.* 103 (2009) 174502.
- [26] C. Lee, C.J. Kim, *Phys. Rev. Lett.* 106 (2011) 014502.
- [27] K. Carpenter, V. Bahadur, *Langmuir* 31 (2015) 2243–2248.
- [28] A. Staicu, F. Mugele, *Phys. Rev. Lett.* 97 (2006) 167801.
- [29] C. Hao, Y. Liu, X. Chen, et al., *Sci. Rep.* 4 (2014) 6846–6852.
- [30] S. Kim, A.A. Polycarpou, H. Liang, *Appl. Surf. Sci.* 351 (2015) 460–465.
- [31] J. Yang, Z. Zhang, X. Men, X. Xu, X. Zhu, *Carbon* 49 (2011) 19–23.
- [32] H.Z. Wang, Z.P. Huang, Q.J. Cai, et al., *Carbon* 48 (2010) 868–875.
- [33] J. Li, J. Ling, L. Yan, et al., *Surf. Coat. Technol.* 258 (2014) 142–145.
- [34] Y. Mo, D. Yan, F. Huang, *Appl. Phys. A* 114 (2013) 1387–1392.
- [35] J. Debgupta, B.A. Kakade, V.K. Pillai, *Phys. Chem. Chem. Phys.* 13 (2011) 14668–14674.
- [36] M.S. Dhindsa, N.R. Smith, J. Heikenfeld, et al., *Langmuir* 22 (2006) 9030–9034.
- [37] X. He, W. Qiang, C. Du, et al., *J. Mater. Chem. A* 5 (2017) 19159–19167.
- [38] N. Vogel, R.A. Belisle, B. Hatton, T.S. Wong, *J. Aizenberg, Nat. Commun.* 4 (2013) 2176–2185.
- [39] P. Kim, M.J. Kreder, J. Alvarenga, J. Aizenberg, *Nano Lett.* 13 (2013) 1793–1799.
- [40] A.G. Papatheanasiou, *Curr. Opin. Colloid Interface Sci.* 36 (2018) 70–77.
- [41] S. Plimpton, *J. Comput. Phys.* 117 (1995) 1–19.
- [42] S.J. Weiner, P.A. Kollman, D.A. Case, et al., *J. Am. Chem. Soc.* 106 (1984) 765–784.
- [43] S. Izadi, A.V. Onufriev, *J. Chem. Phys.* 145 (2016) 074501.
- [44] A.L. Frischknecht, J.G. Curro, *Macromolecules* 36 (2003) 2122–2129.